Inorganic Chemistry

Article

pubs.acs.org/IC

Ternary Borides Cr_2AlB_2, Cr_3AlB_4, and Cr_4AlB_6: The First Members of the Series $(CrB_2)_nCrAl$ with n = 1, 2, 3 and a Unifying Concept for Ternary Borides as MAB-Phases

Martin Ade[†] and Harald Hillebrecht*[,†,‡]

[†]Institut für Anorganische und Analytische Chemie, Albert-Ludwigs-Universität Freiburg, Albertstrasse 21, D-79104 Freiburg, Germany

[‡]Freiburger Materialforschungszentrum FMF, Stefan-Maier-Strasse 25, D-79104 Freiburg, Germany

Supporting Information

ABSTRACT: Single crystals of the ternary borides Cr_2AlB_2, Cr_3AlB_4, Cr_4AlB_6, MoAlB, WAlB, Mn_2AlB_2, and Fe_2AlB_2 were grown from the elements with an excess of Al. Structures were refined by X-ray methods on the basis of single crystal data. All compounds crystallize in orthorhombic space groups. In each case boron atoms show the typical trigonal prisms BM_6. The BM_6-units are linked by common rectangular faces forming B−B-bonds. Thus, zigzag chains of boron atoms are obtained for MoAlB, WAlB, and M_2AlB_2 (M = Cr, Mn, Fe); chains of hexagons for Cr_3AlB_4; and double chains of hexagons for Cr_4AlB_6. The same subunits are known for the binary borides CrB, Cr_3B_4, Cr_2B_3, and β-WB, too. The boride partial structures are separated by single layers of Al-atoms in the case of the chromium compounds and double layers for WAlB, i.e., $W_2Al_2B_2$. All crystal structures can be described using a unified building set principle with quadratic 4^4-nets of metal atoms. The different compositions and crystal structures are obtained by different numbers of metal layers in the corresponding parts according to the formula $(MB)_2Al_y(MB_2)_x$. This principle is an extension of a scheme which was developed for the boridecarbides of niobium. Furthermore, there is a close similarity to the group of ternary carbides $MAl(MC)_n$, so-called MAX-phases. Therefore, they might be named as "MAB-phases". The pronounced two-dimensionality and the mixture of strong covalent and metallic interactions make MAB-phases to promising candidates for interesting material properties. All compositions were confirmed by EDX measurements. Additionally, microhardness measurements were performed.

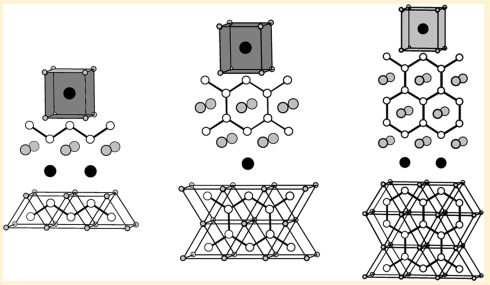

INTRODUCTION

Borides and carbides of the "early" transition metals (i.e., groups 4, 5, and 6) are among the hardest and highest melting compounds.[1−3] These properties have been used for bulk materials or coatings for many purposes for a long time. Recent developments are ruled by two directions. First, binary borides of 5d-metals like ReB_2 and OsB_2 were found to have a remarkably high hardness and/or low compressibility.[4] This is explained by a strong covalent bonding between boron atoms (hardness) and a strong repulsion between the core electrons of the 5d metal (compressibility). Second, so-called "MAX-phases", i.e., ternary carbides and nitrides with the general formula $M_{n+1}AX_n$ (M = Ti, Zr, Hf, V, Nb, Ta, Cr; A = Al, Ga, In, Si, Ge, Sn; X = C, N; n = 1, 2, 3) were found to be unique ceramic materials because they have high thermal, chemical, and mechanical stability in combination with "reversible" plasticity, damage tolerance, and easy machinability.[5] This is explained by the layered structure consisting of a hard carbide or nitride part $(MX)_n$ with variable thickness and a ductile intermetallic part MA.[5] The structures of binary transition metal carbides are usually based on a cubic closest packing of metal atoms with carbon in octahedral voids.[2,6] Frequently, the octahedral sites are partially occupied with less or more pronounced ordering. According to the underlying cubic closest packing the structures are isotropic leading to isotropic material properties for the binary carbides. The pronounced anisotropy of MAX-phases results from the additional intermetallic part. Fundamental differences occur for the transition metal borides. Usually, the structures of borides are based on trigonal prisms BM_6.[6−8] Direct B−B bonds are formed by linkage of common rectangular faces. The further connection is realized by sharing the trigonal basal planes. Therefore, structures and properties of binary borides show high anisotropy. With lower boron content, i.e., M:B > 1, the trigonal prisms BM_6 are isolated (for example, Fe_3B, Co_3B, Ni_3B, Re_3B[6]). With increasing boron content, dimers (Mo_2FeB_2,[9] W_2CoB_2[10]), trimers (W_3CoB_3),[11] tetramers (Mo_2IrB_2,[12] Cr_2IrB_2,[13] $Ti_{1+x}Os_{2-x}RuB_2$[14]), pentamers ($Ni_{12}AlB_8$),[15] and hexamers ($Ti_7Rh_4Ir_2B_8$)[16] are formed, which can be described as fragments of zigzag chains (B_3, B_4, B_5) or layers (B_4, B_6). The high variability results in the existence of many different structure types. With a ratio of 1:1, linear zigzag chains are the dominant feature. The different structure types of monoborides come from the orientation of the chains (CrB-type, parallel and congruent,[17] FeB-type, parallel and fish-bone like,[18]

Received: January 7, 2015
Published: June 12, 2015

DOI: 10.1021/acs.inorgchem.5b00049
Inorg. Chem. 2015, 54, 6122−6135

tetragonal MoB-type (β-MoB) orthogonal[19]), but the motif is still the same. For the binary borides the "transition" between monoborides and diborides with graphite-like layers of hexagons (AlB_2-type) is quite simple (Figure 1). It can be described as a

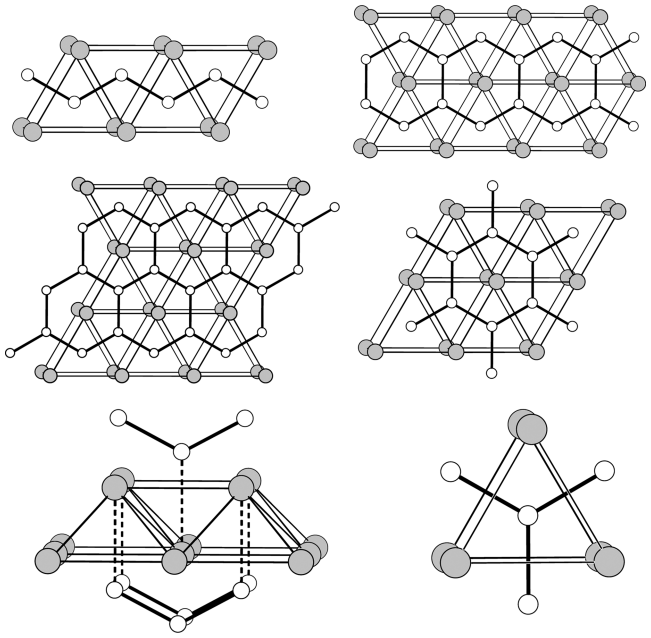

Figure 1. Structures of binary borides: CrB (top, left), Cr_3B_4 (top, right), Cr_2B_3 (middle, left), CrB_2 (middle, right), and the surrounding of boron in CrB (bottom, left) and CrB_2 (bottom, right).

condensation of the chains to double chains (M_3B_4), triple chains (M_2B_3), or a combination of single and double chains (M_5B_6). Further variations of diborides are corrugated layers (WB_2,[20] ReB_2,[21] and the combination of other polygons beyond hexagons (5- and 7- membered rings in $YCrB_4$;[22] 5-, 6-, and 7-membered rings in Y_2ReB_6[23]).

Surprisingly, the complexity in ternary borides with motifs of the boride substructure between monoborides (chains) and diborides (layers) is limited. Parallel single zigzag chains are found for MoAlB[24] and M_2AlB_2 (M = Cr,[25] Mn,[26] Fe[27]), and orthogonal chains in Ru_2ZnB_2.[28] Parallel double chains (i.e., chains of hexagons) are found in Cr_3AlB_4 as the only example.

The material properties of structurally two-dimensional compounds are of high interest as they may act as nanolaminated systems with special crack behavior. In a recent paper, Telle et al.[29] have shown that W_2B_5 (or W_2B_4[20]) exhibits a remarkable similarity to the MAX-phases concerning the mechanical properties (deformation processes, nanodelamination, crack deflection, etc.).

Very recent interest in "MAB-phases" comes from the observation that Fe_2AlB_2 shows a magnetic phase transition around 304 K, making it a prospective magnetocaloric material.[30,31]

In the course of our investigations on the synthetic potential of liquid metals and alloys for synthesis and crystal growth of ternary carbides[32] and borides[33] of transition metals, we have investigated the formation of group 6 borides from liquid aluminum. The focus was on single crystal syntheses for two reasons. While powder data are very suitable for the characterization of the products, single crystal data are essential for the reliable determination of B−B distances because of the low electron number of boron in comparison to the transition metals. Furthermore, the pronounced anisotropy of the crystal structure asks accordingly for the measurement of the microhardness. Using Al as a flux enabled the growth of single crystals. Detailed investigations on single crystals of M/Al/B phases and the characterization of the new compound Cr_4AlB_6 motivated us to a systematic description of these "MAB-phases". Furthermore, we decided to (re)investigate all representatives of "MAB-phases" known in the literature by means of X-ray single crystal diffraction.

EXPERIMENTAL SECTION

Synthesis and Characterization. Single crystals of ternary borides Cr_xAlB_y, MoAlB, WAlB, Mn_2AlB_2, and Fe_2AlB_2 were grown from liquid Al by reaction of the elements. Syntheses were done in corundum crucibles under an atmosphere of argon. Sample sizes were about 3 g of aluminum. Single crystals were isolated from the solidified melt by dissolving the excess of Al in diluted HCl (2 mol/L) with the exception of Mn_2AlB_2 and Fe_2AlB_2. For Mn_2AlB_2 which is less stable against acids a solution of diethyl ether saturated with gaseous hydrogen chloride was used to dissolve the Al-matrix as proposed by Becher et al.[26] For Fe_2AlB_2 which is known to solidify in equilibrium with AlB_2 and Fe_3Al_{14} ("$FeAl_3$") or Fe_2Al_5,[34] single crystals of the ternary boride have been isolated mechanically by crushing the sample.

For the synthesis of the ternary compounds Cr_2AlB_2 and especially Cr_3AlB_4 and Cr_4AlB_6 slow cooling is essential. Okada et al. obtained the binary chromium borides from liquid Al[35] with similar ratios of the elements in the same temperature regime, but with a cooling rate of 50 K/h.

Cr_2AlB_2. Single crystals of Cr_2AlB_2 are easily obtained from a ratio Cr:B:Al of 1:1:30 by cooling down the samples at 10 °C/h from 1500 to 800 °C. X-ray powder diffraction showed Cr_2AlB_2 as main phase and CrB as a minor product (S1). Single crystals of Cr_2AlB_2 crystallize as laths (Figure 2).

Cr_3AlB_4. Cr_3AlB_4 was obtained from a ratio Cr:B:Al of 1:1.33:30. The educts were heated with 300 °C/h to 1000 °C, annealed for 72 h at 1000 °C, and then cooled with 50 °C increments to room temperature. The annealing step is essential, because Cr_3AlB_4 decomposes above 1100 °C to the binary borides Cr_3B_4 and Cr_2B_3. The X-ray powder diffraction diagram showed Cr_3AlB_4 as the main product with very small amounts of Cr_3B_4 (Supporting Information Figure S2). Crystals were obtained as laths similar to Cr_2AlB_2, but also thicker prisms have been observed (Figure 2). With increased boron amount (1:1.5:30) Cr_2B_3 was found as a second phase.

Cr_4AlB_6. Cr_4AlB_6 was obtained from a ratio Cr:B:Al of 1:1.55:30 with the same temperature conditions as those used for Cr_3AlB_4. Similar to the procedure for Cr_3AlB_4, the annealing step is essential. Single crystals were formed as laths (Figure 2). The powder XRD (Supporting Information Figure S3) showed Cr_3AlB_4 as a byproduct. It should be mentioned that attempts to synthesize Cr_4AlB_6 are not successful in all cases but can lead to other binary or ternary borides instead of Cr_4AlB_6.

MoAlB. Single crystals of MoAlB are obtained in the system Mo/Al/B (excess Al) over a quite extended range of compositions. Typical conditions are heating to 1500 °C, annealing for 24 h, and then coolimg with 10 °C/h to 800 °C. The ratio Mo:B:Al was varied between 1:1:30 and 1:1:150. Well-developed single crystals with a length up to several millimeters were isolated (Figure 2). The X-ray powder diagram of crushed single crystals corresponded to the calculated pattern of MoAlB (Supporting Information Figure S4). Single crystals of orthorhombic MoB (α-MoB) were found as a byproduct. Because there are no current structural data[6] on the basis of single crystal data we carried out a refinement.

WAlB. A few single crystals of WAlB were obtained as byproducts from batches containing W, B, and Al in different amounts (W:B:Al between 1:1:30 and 1:1:150; W:B between 2:3 and 3:2). Slow cooling rates were essential to obtain WAlB (heating to 1550 °C, annealing for 24 h, cooling with 2 °C/h to 660 °C). According to investigations by powder and single crystal methods the main products were the intermetallics WAl_{12},[6,36] WAl_6,[36] WAl_5,[6,36] and tetragonal WB (β-WB)[37]

DOI: 10.1021/acs.inorgchem.5b00049
Inorg. Chem. 2015, 54, 6122−6135

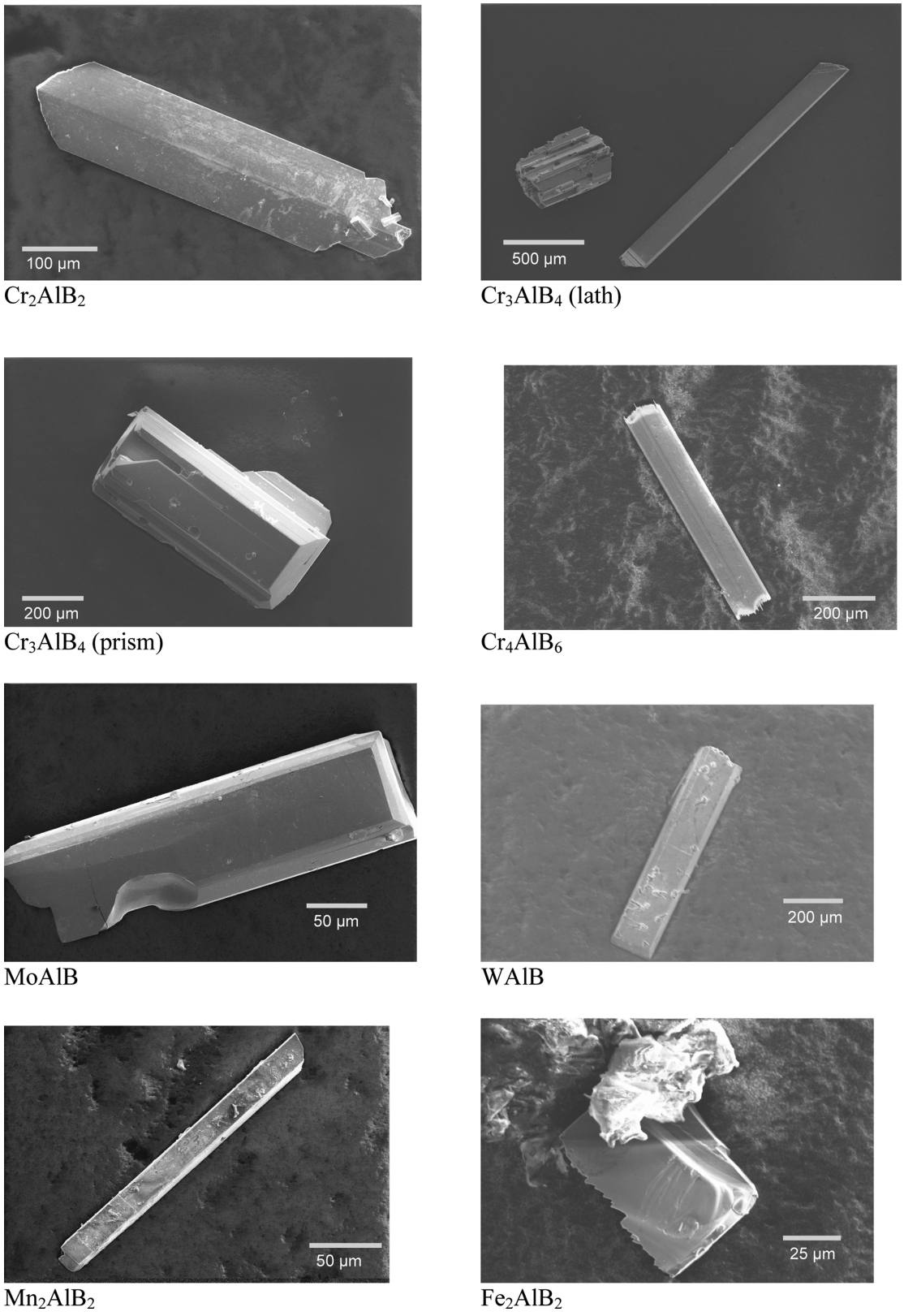

Figure 2. REM pictures of MAB-phases.

depending on the ratios chosen. Single crystals of the latter are formed in different shapes, but checks with XRD always revealed β-WB. Single crystals of WAlB were obtained as small coffin-like rods (Figure 2). X-ray powder diagrams from batches with significant amounts of WAlB were indexed and assigned according to the data obtained from single crystal investigations (Supporting Information Figure S5). Numerous attempts for the synthesis of WAlB described by Okada et al.[38] did not result in higher amounts. It should be mentioned that despite the close similarity of the binary phase diagrams Mo/B–W/B and Mo/Al–W/Al the tendency to form MoAlB and WAlB is different.

Mn_2AlB_2. Mn_2AlB_2 could be synthesized from melts in the Mn/Al/B system with atomic ratios Mn:Al:B between 1:1:10 and 1:1:30 by

DOI: 10.1021/acs.inorgchem.5b00049
Inorg. Chem. 2015, 54, 6122–6135

Table 1. Structure Refinement of Cr_2AlB_2, Cr_3AlB_4, Cr_4AlB_6, WAlB, MoAlB, Mn_2AlB_2, Fe_2AlB_2, and MoB

	Cr_2AlB_2	Cr_3AlB_4	Cr_4AlB_6	MoAlB
cryst shape	flat rod	flat rod	flat rod	coffin-like rod
cryst color	metallic lustrous	metallic lustrous	metallic lustrous	metallic lustrous
cryst size	0.02 × 0.04 × 0.3 mm^3	0.015 × 0.05 × 0.25 mm^3	0.02 × 0.05 × 0.35 mm^3	0.03 × 0.05 × 0.25 mm^3
fw	76.30 g/mol	113.11 g/mol	299.54 g/mol	177.49 g/mol
cryst syst	orthorhombic	orthorhombic	orthorhombic	orthorhombic
space group	*Cmmm*	*Pmmm*	*Cmmm*	*Cmcm*
lattice constants	a = 2.9373(3) Å	a = 2.9556(4) Å	a = 2.9517(4) Å	a = 3.1987(4) Å
	b = 11.0513(12) Å	b = 2.9778(5) Å	b = 21.280(3) Å	b = 13.9218(14) Å
	c = 2.9675(3) Å	c = 8.0539(14) Å	c = 3.0130(3) Å	c = 3.0937(3) Å
cell volume	96.33 $Å^3$	70.88 $Å^3$	189.26 $Å^3$	137.77 $Å^3$
formula units	2	1	2	2
density, calcd	5.26 g/cm^3	5.30 g/cm^3	5.26 g/cm^3	6.45 g/cm^3
radiation	Mo Kα	Mo Kα	Mo Kα	Mo Kα
θ-range	$-6 \le h \le 6$, $-23 \le k \le 0$, $-6 \le l \le 6$	$-4 \le h \le 4$, $-4 \le k \le 4$, $-12 \le l \le 12$	$-4 \le h \le 4$, $-34 \le k \le 34$, $-4 \le l \le 4$	$-5 \le h \le 5$, $-22 \le k \le 22$, $-5 \le l \le 5$
$2\theta_{max}$	100°	70°	70°	72°
diffractometer	CAD4	STOE IPDS II	STOE IPDS II	STOE IPDS II
data collection	$\omega/2\Theta$-scan	$0° \le \omega \le 180°$;	$0° \le \omega \le 180°$;	$0° \le \omega \le 180°$;
	0.80° ± 0.50 tan Θ	φ = 0°, $\Delta\omega$ = 2°	φ = 0°, $\Delta\omega$ = 2°	φ = 0°, 111°, $\Delta\omega$ = 2°
measure time	60 s	180 s	360 s	180 s
reflns measured	1041	1557	1879	1574
indep reflns	325	214	278	211
reflns $I > 2\sigma(I)$	307	183	208	199
abs corr	numerical, ψ-scan	equivalent, program XAREA/XSHAPE[42,43]	equivalent, program XAREA/XSHAPE[42,43]	equivalent, program XAREA/XSHAPE[42,43]
max/min transm	0.644; 0.363	0.632; 0.388	0.642; 0.421	0.1321; 0.0886
R_{int}, R_σ	0.0370, 0.0264	0.0880, 0.0338	0.0631; 0.0359	0.071, 0.021
abs coeff	11.22 mm^{-1}	11.28 mm^{-1}	11.19 mm^{-1}	9.39 mm^{-1}
extinction coeff[41]	0.400(14)	0.028(14)	0.045(2)	0.103(6)
residual electron $e^-/Å^3$ min, max, σ	+1.08, −0.89, 0.20	+0.72, −0.77, 0.18	+0.75, −0.90, 0.19	+0.80, −1.44, 0.22
weighting function[41]	0.0118; 0.0	0.0374; 0.0	0.011; 1.15	0.029; 0.0
no. params	13	20	25	14
R-factors	R1(F) = 0.0135	R1(F) = 0.0193	R1(F) = 0.0256	R1(F) = 0.0145
	wR2(F^2) = 0.0304	wR2(F^2) = 0.0474	wR2(F^2) = 0.0414	wR2(F^2) = 0.0379
	WAlB	Mn_2AlB_2	Fe_2AlB_2	MoB
cryst shape	flat needle	flat needle	irregular fragment	Small rod
cryst color	metallic lustrous	metallic lustrous	black lustrous	black
cryst size	0.02 × 0.05 × 0.4 mm^3	0.1 × 0.05 × 0.2 mm^3	0.1 × 0.15 × 0.2 mm^3	0.05 × 0.05 × 0.1 mm^3
fw	221.64 g/mol	79.24 g/mol	80.15 g/mol	106.75 g/mol
cryst syst	orthorhombic	orthorhombic	orthorhombic	orthorhombic
space group	*Cmcm*	*Cmmm*	*Cmmm*	*Cmcm*
lattice constants	a = 3.2016(3) Å	a = 2.9180(4) Å	a = 2.9217(4) Å	a = 3.1418(2) Å
	b = 13.9059(12) Å	b = 11.038(2) Å	b = 10.991(15) Å	b = 8.4961(6) Å
	c = 3.1020(2) Å	c = 2.8932(5) Å	c = 2.8563(5) Å	c = 3.0721(2) Å
cell volume	138.10 $Å^3$	93.19 $Å^3$	91.79 $Å^3$	82.00 $Å^3$
formula units	2	2	2	4
density, calcd	10.66 g/cm^3	5.65 g/cm^3	5.80 g/cm^3	8.65 g/cm^3
radiation	Mo Kα	Mo Kα	Mo Kα	Mo Kα
θ-range	$-4 \le h \le 4$, $-20 \le k \le 20$, $0 \le l \le 4$	$-4 \le h \le 4$, $-17 \le k \le 17$, $-4 \le l \le 4$	$-4 \le h \le 4$, $-17 \le k \le 17$, $-4 \le l \le 4$	$-5 \le h \le 5$, $-10 \le k \le 14$, $0 \le l \le 5$
$2\theta_{max}$	66°	70°	70°	72°
diffractometer	STOE IPDS II	STOE IPDS II	STOE IPDS II	CAD4
data collection	$0° \le \omega \le 180°$;	$0° \le \omega \le 180°$;	$0° \le \omega \le 180°$;	$\omega/2\Theta$-scan
	φ = 0°, 111°, $\Delta\omega$ = 2°	φ = 0°, 111°, $\Delta\omega$ = 2°	φ = 0°, 111°, $\Delta\omega$ = 2°	0.80° ± 0.50 tan Θ
measure time	300 s	240 s	240 s	60 s
reflns measured	1768	1406	1106	256
indep reflns	167	145	138	120
reflns $I > 2\sigma(I)$	160	140	120	117
abs corr	empirical, program XAREA/XSHAPE[42,43]	empirical, program XAREA/XSHAPE[42,43]	empirical, program XAREA/XSHAPE[42,43]	numerical, ψ-scan
max/min transm	0.3052; 0.0659	0.467; 0.250	0.337; 0.186	0.534; 0.330

DOI: 10.1021/acs.inorgchem.5b00049
Inorg. Chem. 2015, 54, 6122−6135

Table 1. continued

	WAlB	Mn_2AlB_2	Fe_2AlB_2	MoB
R_{int}, R_σ	0.076, 0.026	0.073, 0.032	0.068, 0.027	0.043 ; 0.034
abs coeff	85.06 mm^{-1}	13.48 mm^{-1}	15.74 mm^{-1}	14.67 mm^{-1}
extinction coeff[41]	0.014(1)	0.16(2)	0.094(8)	0.032(9)
residual electron $e^-/Å^3$ min, max, σ	+1.18, −2.17, 0.38	+1.46, −0.79, 0.21	+0.79, −0.73, 0.16	+2.16, −2.47, 0.44
weighting function[41]	0.009; 0.0	0.045; 0.0	0.020; 0.0	0.040; 1.085
no. params	12	13	13	10
R-factors	R1(F) = 0.0140	R1(F) = 0.0229	R1(F) = 0.0162	R1(F) = 0.0254
	wR2(F^2) = 0.0294	wR2(F^2) = 0.0542	wR2(F^2) = 0.0359	wR2(F^2) = 0.0657

Table 2. Coordinates, Displacement Parameters (in 10^4 $Å^2$), and Site Occupation Factors[a]

compd atom	site	x	y	z	U_{eq}	sof[b]	U_{11}	U_{22}	U_{33}
				Cr_2AlB_2					
Cr	4*i*	0	0.146 86(1)	0	24(1)	1.003(3)	28(1)	30(1)	14(1)
Al	2*c*	0	0.5	0.5	40(1)	0.99(2)	51(2)	32(1)	36(1)
B	4*j*	0	0.294 01(8)	0.5	38(1)	1.006(6)	37(3)	48(3)	28(2)
				Cr_3AlB_4					
Cr1	1*a*	0	0	0	64(2)	1.001(6)	67(3)	56(3)	68(3)
Cr2	2*f*	0	0	0.29923(7)	51(2)	1.002(6)	49(2)	40(2)	64(2)
Al	1*b*	0	0	0.5	68(3)	0.99(1)	73(6)	76(5)	54(5)
B1	2*f*	0	0.5	0.1077(5)	62(5)	1.00(2)	55(12)	54(12)	77(15)
B2	2*a*	0	0	0.2214(5)	58(5)	1.01(2)	58(11)	51(11)	69(13)
				Cr_4AlB_6					
Cr1	4*i*	0	0.076 34(4)	0	34(2)	0.998(1)	25(4)	47(4)	41(4)
Cr2	4*i*	0	0.688 43(4)	0	51(2)	0.999(1)	42(4)	57(4)	55(4)
Al	2*c*	0	0.5	0.5	63(4)	1.01(2)	65(9)	44(9)	80(10)
B1	4*j*	0	0.6050(2)	0.5	40(11)	0.99(4)	31(23)	16(19)	73(27)
B2	4*j*	0	0.1481(3)	0.5	62(11)	1.00(4)	60(24)	10(18)	115(28)
B3	4*j*	0	0.2298(2)	0.5	53(13)	1.04(4)	81(32)	24(20)	52(31)
				WAlB					
W	4*c*	0	0.410 02(2)	0.25	36(2)	0.99 (1)	33(2)	40(2)	34(2)
Al	4*c*	0	0.3006(2)	0.25	62(5)	1.06(2)	53(13)	70(10)	61(10)
B	4*c*	0	0.4645(6)	0.25	33(14)[c]	1.13(7)			
				MoAlB					
Mo	4*c*	0	0.410 52(2)	0.25	34(1)	0.99(1)	40(2)	31(2)	30(2)
Al	4*c*	0	0.198 49(9)	0.25	61(2)	1.01(1)	70(5)	46(4)	66(5)
B	4*c*	0	0.0338(3)	0.25	53(6)	0.98(4)	51(13)	68(14)	39(14)
				Mn_2AlB_2					
Mn	4*i*	0	0.144 91(5)	0	48(2)	1.00(1)	41(2)	56(3)	46(3)
Al	2*c*	0	0.5	0.5	58(3)	1.01(1)	57(6)	45(6)	72(6)
B	4*j*	0	0.2937(3)	0.5	60(6)	0.95(3)	37(13)	80(16)	62(13)
				Fe_2AlB_2					
Fe	4*i*	0	0.145 96(5)	0	66(2)	0.962(9)	81(2)	58(2)	61(2)
Al	2*c*	0	0.5	0.5	67(3)	1.04(1)	79(6)	36(6)	85(6)
B	4*j*	0	0.2932(3)	0.5	81(6)	1.04(3)	81(14)	76(14)	88(13)
				MoB					
Mo	4*c*	0	0.854 84(6)	0.25	48(3)	1.02(2)	59(2)	59(4)	60(4)
B	4*c*	0	0.5601(9)	0.25	97(13)	0.85(8)	76(28)	92(26)	124(34)

[a] esd's in parentheses, $U_{12} = U_{23} = U_{13} = 0$. [b] In order to check for mixed occupations and/or vacancies, site occupation factors were treated by turns as free variables at the end of the refinement. [c] U_{iso}.

cooling the melts from 1450 to 800 °C with 10 °C/h increments. Laths of Mn_2AlB_2 (Figure 2) have been obtained after dissolving the excess Al with diethyl ether saturated by gaseous hydrogen chloride. The powder XRD (Supporting Information Figure S6) showed $MnAl_6$ and AlB_2 as byproducts. A polished section of the solidified melt (Supporting Information Figure S8) showed $MnAl_6$ and Al beside Mn_2AlB_2.

Fe_2AlB_2. Fe_2AlB_2 could be synthesized from melts in the system Fe/Al/B with an atomic ratio Fe:Al:B of 3:3:4 and the same temperature conditions as for Mn_2AlB_2. Powder XRD of the sample (Supporting Information Figure S7) showed Fe_2AlB_2 as the main phase with smaller amounts of Fe_4Al_{13}.[6] EDX measurements of polished sections of the solidified melt (Supporting Information Figure S8) revealed also the presence of $(Al_{1-x}Fe_x)B_2$ (EDX: $x \approx 0.05$) and α-AlB_{12}[6] in the samples. Because Fe_2AlB_2 reacts with hydrochloric acid, single crystals (Figure 2) were isolated mechanically after crushing the solidified samples.

Structure Analysis. Single crystals were selected under a microscope from the residues after dissolving the material. Different types of single crystal diffractometers were used for data collection (see Table 1). Indexing procedures resulted in orthorhombic unit cells. For MoAlB, WAlB, Cr_2AlB_2, Cr_3AlB_4, Mn_2AlB_2, and Fe_2AlB_2, observed lattice

DOI: 10.1021/acs.inorgchem.5b00049
Inorg. Chem. 2015, 54, 6122−6135

Table 3. Selected Distances (Å) and Angles (deg), with esd's in Parentheses

Cr_2AlB_2					
Cr−B	2.1876(3) 4×	Al−B	2.2765(9) 2×	B−B	1.7616(9) 2×
−B	2.2014(6) 2×	−Cr	2.6643(2) 8×	−Cr	2.1876(3) 4×
−Al	2.6443(2) 4×	−Al	2.9372(3) 2×	−Cr	2.2014(6) 2×
−Cr	2.7118(2) 2×	−Al	2.9675(3) 2×	−Al	2.2765(9) 1×
−Cr	2.9372(3) 2×			B−B−B	113.0(1)
−Cr	2.9675(3) 2×				
−Cr	3.2460(2)				
Cr_3AlB_4					
Cr2−B1	2.144(3) 2×	Al−B2	2.244(4) 2×	B1−B1	1.735(8)
−B2	2.190(1) 4×	−Cr2	2.6487(4) 8×	−B2	1.738(3) 2×
−Al	2.6487(4) 4×	−Al	2.9556(4) 2×	B2−Al	2.244(4)
−Cr1	3.236(1)	−Al	2.9778(5) 2×		
Cr1−B1	2.270(2) 8×			B2−B1−B2	116.4(3)
−B2	2.323(3) 4×			B1−B1−B2	121.8(1)
−Cr2	2.826(1) 4×				
Cr_4AlB_6					
Cr1−B1	2.146(4) 2×	Al−B1	2.234(5) 2×	B1−B2	1.738(4) 2×
−B2	2.195(1) 4×	−Cr1	2.6621(5) 8×	−Al	2.234(5)
−Al	2.6621(5) 4×	−Al	2.9517(4) 2×	B2−B3	1.738(7)
Cr2−B2	2.277(2) 4×	−Al	3.0130(3) 2×	−B1	1.738(4) 2×
−B3	2.285(2) 4×			B3−B3	1.707(5) 2×
−B3	2.301(4) 2×			−B2	1.738(7)
−B1	2.329(4) 2×			B2−B1−B2	116.2(4)
				B1−B2−B1	116.2(4)
				B1−B2−B3	121.9(2)
				B2−B3−B3	119.6(6)
				B3−B3−B3	120.2(3)
MoAlB					
Mo−B	2.346(3) 4×	Al−B	2.293(4)	B−B	1.810(4) 2×
−B	2.356(1) 2×	−Mo	2.6933(7) 4×	−Mo	2.346(3) 4×
−Al	2.6933(7) 4×	−Mo	2.952(1)	− Mo	2.356(1) 2×
−Al	2.952(1)	−Al	2.647(1) 4×	−Al	2.293(4)
−Mo	2.9325(5) 2×			B−B−B	117.4(13)
WAlB					
W−B	2.354(3) 4×	Al−B	2.280(9)	B−B	1.838(9) 2×
−B	2.368(6) 2×	−W	2.699(2) 4×	−W	2.354(3) 4×
−Al	2.699(2) 4×	−W	2.928(3)	−W	2.368(6) 2×
−Al	2.929(3)	−Al	2.636(3) 4×	−Al	2.280(9)
−W	2.944(1) 2×			B−B−B	115.1(9)
Mn_2AlB_2					
Mn−B	2.164(1) 4×	Al−B	2.277(4) 2×	B−B	1.749(4) 2×
−B	2.188(3) 2×	−Mn	2.604(1) 8×	−Mn	2.164(1) 4×
−Al	2.6038(4) 4×	−Al	2.8932(5) 2×	−Mn	2.188(3) 2×
−Mn	2.741(1) 2×	−Al	2.9180(4) 2×	−Al	2.277(4) 1×
−Mn	2.8932(5) 2×			B−B−B	113.1(4)
−Mn	2.9180(4) 2×				
−Mn	3.1990(4)				
Fe_2AlB_2					
Fe−B	2.150(1) 4×	Al−B	2.275(4) 2×	B−B	1.742(4) 2×
−B	2.159(3) 2×	−Fe	2.5983(4) 8×	−Fe	2.150(1) 4×
−Al	2.5983(4) 4×	−Al	2.8563(5) 2×	−Fe	2.159(3) 2×
−Fe	2.715(1) 2×	−Al	2.9217(4) 2×	−Al	2.275(4) 1×
−Fe	2.8563(5) 2×			B−B−B	113.9(4)
−Fe	2.9217(4) 2×				
−Fe	3.2111(3)				
MoB					
Mo−B	2.313(2) 4×	Mo−Mo	2.8285(6) 4×	B−B	1.844(9) 2×
−B	2.347(6) 2×	−Mo	2.9058(8) 2×	−Mo	2.313(2) 4×
−B	2.505(8)	−Mo	3.0721(2) 2×	−Mo	2.347(6) 2×
		−Mo	3.1418(2) 2×	B−B−B	112.8(9)

DOI: 10.1021/acs.inorgchem.5b00049
Inorg. Chem. 2015, 54, 6122−6135

Table 4. EDX Measurements on MAB-Phases

compd composition		wt % TM	wt % Al	wt % B	at. % TM	at. % Al	at. % B	standards
Cr_2AlB_2	theor	68.15	17.68	14.17	40.0	20.0	40.0	
$Cr_{2.00}Al_{1.02}B_{1.99}$	expt	68.0(4)	17.9(4)	14.0(4)	39.7(2)	20.3(5)	40(1)	Cr_7**Al**$_{45}$ ext, **Cr**$_3$**B**$_4$ ext
Cr_3AlB_4	theor	68.96	11.93	19.11	37.5	12.5	50.0	
$Cr_{2.83}Al_{0.98}B_{4.19}$	expt	67.2(4)	12.1(2)	20.7(4)	35.4(2)	12.3(2)	52(1)	Cr_7**Al**$_{45}$ ext, **Cr**$_3$**B**$_4$ ext
Cr_4AlB_6	theor	68.96	11.93	19.11	45.4	9.1	54.5	
$Cr_{2.83}Al_{0.98}B_{4.19}$	expt	67.2(4)	12.1(2)	20.7(4)	67.2(4)	12.1(2)	20.7(4)	Cr_7**Al**$_{45}$ ext, **Cr**$_3$**B**$_4$ ext
MoAlB	theor	71.74	20.07	8.08	33.3	33.3	33.3	
$Mo_{1.10}Al_{0.84}B_{1.06}$	expt	72.4(6)	16.8(2)	10.8(7)	36.6(3)	28.1(3)	35(2)	Mo int, **Al**$_2$O$_3$ int, Cr_3**B**$_4$ ext
WAlB	theor	82.95	12.17	4.88	33.3	33.3	33.3	
$W_{1.03}Al_{1.02}B_{0.95}$	expt	83.4(5)	12.1(1)	4.5(5)	34.4(2)	34.0(3)	32(3)	Cr_2**B**$_3$ ext, **Al**$_2$O$_3$ int, **W** int
Mn_2AlB_2	theor	69.33	17.02	13.64	40.0	20.0	40.0	
$Mn_{2.03}Al_{0.97}B_{2.01}$	expt	70.0(9)	16.4(4)	13.6(8)	40.5(5)	19.4(5)	40(2)	Cr_2**B**$_3$ ext, **Al**$_2$O$_3$ int, **Mn** int
Fe_2AlB_2	theor	69.68	16.83	13.49	40.0	20.0	40.0	
$Fe_{2.10}Al_{0.97}B_{1.93}$	expt	71.5(6)	15.9(5)	12.7(9)	42.1(4)	19.4(6)	39(3)	Cr_2**B**$_3$ ext, **Al**$_2$O$_3$ int, **Fe** int

Table 5. Refined Lattice Parameters of MAB-Phases from Powder-XRD with Values in Å[a]

compd	this work: single crystal	this work: powder	reference	reference	reference
Cr_2AlB_2			ref 25	ref 31	
a	2.9373(3)	2.939(1)	2.937	2.949(6)	
b	11.051(1)	11.054(3)	11.07	11.10(1)	
c	2.9675(3)	2.968(1)	2.971	2.948(5)	
V	96.33	96.43(7)	96.59	96.53(1)	
Cr_3AlB_4			ref 25		
a	2.9556(4)	2.9506(7)	2.989		
b	2.9778(5)	2.9851(7)	2.952		
c	8.054(1)	8.083(2)	8.091		
V	70.88	71.21(3)	71.39		
Cr_4AlB_6					
a	2.9517(5)	2.9432(9)			
b	21.280(3)	21.225(9)			
c	3.0130(3)	3.003(1)			
V	189.26	187.6(2)			
Fe_2AlB_2			ref 27a	ref 27b	ref 30
a	2.9217(4)	2.9263(5)	2.923(1)	2.923(2)	2.9311(2)
b	10.999(2)	11.036(2)	11.034(1)	11.046(5)	11.0376(3)
c	2.8563(5)	2.8667(5)	2.8703(3)	2.875(2)	2.8783(2)
V	91.79	92.58(2)	92.58	92.83	93.119(2)
Mn_2AlB_2			ref 26	ref 31	
a	2.9180(4)	2.9259(8)	2.92	2.936(5)	
b	11.038(2)	11.080(4)	11.08	11.12(1)	
c	2.8932(5)	2.9016(9)	2.89	2.912(8)	
V	93.19	94.07(7)	93.50	95.06(1)	
MoAlB			ref 24	ref 55	
a	3.1987(4)	3.2112(3)	3.212(2)	3.2085(3)	
b	13.922(1)	13.977(1)	13.985(4)	13.980(1)	
c	3.0937(3)	3.1024(3)	3.102(1)	3.1002(3)	
V	137.77	139.24(3)	139.34	139.06	
WAlB			ref 38		
a	3.2065(9)	3.202(2)	3.205(1)		
b	13.919(3)	13.925(5)	13.947(2)		
c	3.1051(8)	3.096(4)	3.108(1)		
V	138.59	138.0(3)	138.9(1)		

[a]For experimental and calculated diagrams see Supporting Information Figures S1−S7.

parameters and reflection conditions were characteristic for the structure types MoAlB,[24] Mn_2AlB_2,[26] (revised space group[39]) and Cr_3AlB_4.[25] Therefore, the corresponding space groups and structural parameters were used as a model for starting the refinements. Quick convergence confirmed its correctness. The refinement of the site occupation factors revealed no significant deviations from a stoichio-

DOI: 10.1021/acs.inorgchem.5b00049
Inorg. Chem. 2015, 54, 6122−6135

metric composition. The excellent *R*-values indicate the high quality of the crystals. For Cr_4AlB_6 the size of the lattice parameters and the reflection conditions ($h + k = 2n$) indicated a new phase. According to the knowledge on binary borides the first assumption was a compound Cr_5B_6 with a V_5B_6-type structure (*Cmmm*, a = 2.97 Å, b = 21.24 Å, c = 3.06 Å).[40] The refinement of the corresponding structure model showed some significant deviations (one B atom on a different site, one Cr-atom with "reduced" electron density). Therefore, the composition Cr_4AlB_6 was assumed and confirmed by a successful refinement. All site occupation factors were checked for mixed or partial occupations, but no significant deviations were found.

Structure solution and refinements were done using the program package SHELXL.[41] Further details of all refinements are listed in Table 1−3. Details of the structure refinement (complete list of distances and angles, $I/\sigma(I)$-list) may be obtained from Fachinformationszentrum Karlsruhe, D-76344 Eggenstein-Leopoldshafen (Germany) (fax, +49)724-808-666; e-mail, crysdata@fiz-karlsruhe.de) on quoting the registry numbers CSD-427198 (Cr_2AlB_2), 427199 (Cr_3AlB_4), 427200 (Cr_4AlB_6), 427203 (MoAlB), 427204 (WAlB), 427201 (Mn_2AlB_2), 427202 (Fe_2AlB_2), and 427755 (α-MoB).

SEM/EDX. High reaction temperatures and high reactivity of the melt can lead to unexpected contaminations (crucible, metallic melt, starting material). Therefore, all single crystals were additionally analyzed by energy dispersive X-ray spectroscopy (EDX). In each case only the expected elements were detected in agreement with the X-ray results. SEM pictures of the single crystals are shown in Figure 2. For EDX measurements well-grown single crystals of Cr_2AlB_2, Cr_3AlB_4, Cr_4AlB_6, and WAlB were cleaned by rinsing with water, ethanol, and toluene and measured without further surface modifications, while for MoAlB, Mn_2AlB_2, and Fe_2AlB_2 EDX measurements showed an enhanced oxygen content on the crystal surfaces or the surfaces were not smooth enough for reliable quantitative element determinations. Therefore, these samples were embedded in epoxy resin and polished to obtain clean smooth surfaces.

EDX measurements were done with a LEO 1525 scanning electron microscope and an Oxford/Link EDX device with X-Max SDD-Detector at the Institut für Kristallographie (University of Freiburg). A low acceleration voltage of 10 kV was used to enhance the precision of the boron determination near the heavier elements. For each sample 5−12 point measurements (60 s) were carried out, and the results merged. Cr_3B_4 and Cr_2B_3 single crystals were used as external standards for boron and chromium, and Cr_7Al_{45} crystals were used as Al standard in the case of Cr_2AlB_2, Cr_3AlB_4, and Cr_4AlB_6. Internal standards were used for all other elements. Data processing and corrections were done using the Oxford/Link INCA software (Version 4.15). The following lines were used: K-line, B, Al, Mn, and Fe; L-line, Cr, Mo; M-line, W. The results fit well to the experiences from other analyses of light elements.[44]

Table 4 shows the results of the EDX measurements. The quantitative determination of boron besides the heavy elements Mo and especially W requires careful standardization. Excellent values are found for Cr_2AlB_2, WAlB, and Mn_2AlB_2, and good agreement for Cr_3AlB_4 and Fe_2AlB_2. Larger deviations (excess of Mo, deficit of Al) are found for MoAlB. This difference proceeded although several crystals were measured and different techniques used for preparation and calibration. The results of the refinement give no hints for the observed deviation so the reason remains unclear.

Powder XRD. All samples were characterized by powder XRD. Experimental and calculated patterns are shown in the Supporting Information Figures S1−S7. Patterns were recorded with a STOE Stadi P (Cu Kα1 radiation, Ge monochromator, image plate detector, Debye−Scherrer geometry, transmission).

Refined lattice parameters are listed in Table 5.

Microhardness. Microindentation hardness testing was performed using a microhardness equipment MHT 10 (producer: A. Paar, Austria). A force of 1 N was generated within 10 s and applied for 15 s. The square pyramid imprints of the Vickers indenter were evaluated and converted into a microindentation hardness value H_V according to the usual procedures.[45]

RESULTS

Cr_2AlB_2. The crystal structure of Cr_2AlB_2 (Figure 3a) belongs to the Mn_2AlB_2-type,[26] which was first described in space group

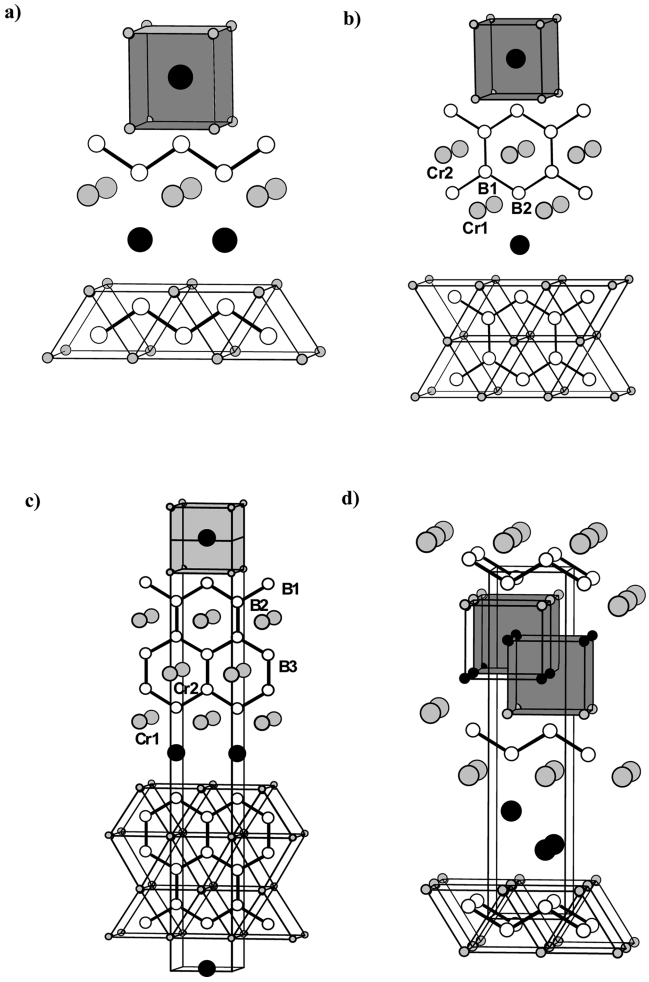

Figure 3. Crystal structures of (a) Cr_2AlB_2 (view along [001]), (b) Cr_3AlB_4 (view along [001]), (c) Cr_4AlB_6 (view along [001]), (d) MoAlB view along [100]): white, B; black, Al; gray, Cr/Mo.

*C*222, but later corrected to *Cmmm*.[39] This confirms the data of Chaban and Kuz'ma.[25b] In Cr_2AlB_2 the B atoms show the typical trigonal-prismatic coordination with very similar B−Cr-distances of 2.188 Å (2×) and 2.201 Å (4×). The prisms are connected by rectangular faces common to linear rods. According to the short distances of the prism centers there are B−B distances of 1.762 Å forming a zigzag chain (B−B−B: 113°). This value corresponds to a usual single bond (covalent radius r_B = 0.88 Å) and is significantly longer than that given by Chaban and Kuz'ma (1.612 Å). The zigzag chains are linked to layers by the triangles of the prisms. The third rectangular side is capped by Al (B−Al: 2.276 Å), thus linking the layers to a three-dimensional structure. The resulting coordination of Al corresponds to the pattern of a bcc packing (CsCl-type) with 8 Cr (2.644 Å), 2 B (2.276 Å), and 4 Al (2.937−2.968 Å). A similar array is found for the HT-forms of the alloys $Cr_{0.67}Al_{0.33}$ and $Cr_{0.78}Al_{0.22}$.[46] Also, LT-$AlCr_2$ ($MoSi_2$-type)[47] and Al_8Cr_5 (γ-brass)[48] show a similarity to bcc. The surrounding of Cr reflects the arrangement of the metal 4^4-nets (see below). Four longer distances (2.937−2.968 Å), which correspond to the pseudotetragonal lattice parameters a and c, constitute the 4^4-net. Two shorter distances (2.712 Å) result

DOI: 10.1021/acs.inorgchem.5b00049
Inorg. Chem. 2015, 54, 6122−6135

from the next net within the boride part and additionally four Al-atoms (2.644 Å) from the net of Al-atoms. The coordination is completed by six B atoms. The $AlCr_8$-cubes of the bcc-packing are elongated in the *b*-direction (10%) that enlarges the Cr−Cr distance to 3.246 Å. All distances are comparable to other well-known binary compounds and show no peculiarities.

Cr_3AlB_4. Cr_3AlB_4 was already described in 1972 by Kuz'ma et al.[25] The crystal structure (Figure 3b) was derived from powder data, crystal chemical considerations, and a trial-and-error refinement. This model was confirmed and rendered more precisely by the present investigations (for example, B−B distances were given as 1.707−1.715 Å in ref 25).

All B atoms form trigonal prisms BCr_6. The rectangular faces are capped by three B atoms (B1) or two boron and one Al atom (B2). Al and one of the two independent Cr atoms show the same features as those in Cr_2AlB_2. The hexagonal prismatic coordination of the second Cr atom (Cr2) shows the relation to the hexagonal CrB_2 (AlB_2-type). This can be easily explained by combination of two of the zigzag chains like those in Cr_2AlB_2 to a linear chain of B_6 hexagons as found in Cr_3B_4. Now the "central" atoms B1 and Cr2 in Cr_3AlB_4 represent a cut-out of the AlB_2-type with layers of planar boron hexagons and hexagonal prismatic coordination of the metal atoms. The deviations are very small. The B−B distances are between 1.735 and 1.738 Å; the B−B−B angles are between 116 and 122°. The distances Cr1−B are between 2.270 and 2.322 Å. According to the structural features, B−B and Cr−B distances are similar to those in CrB_2 with 1.721 Å (B−B) and 2.320 Å (Cr−B).[47] The distances Cr2−B are significantly shorter (2.144/2.190 Å) but comparable to those in Cr_2AlB_2.

Al is located between the layers of the Cr/B partial structure. The bcc-analogous arrangement known from Cr_2AlB_2 is continued with only small changes (Al−B slightly shorter, Al−Al and Al−Cr distances longer). The elongation in direction of the layer stacking is confirmed.

Cr_4AlB_6. The structure of Cr_4AlB_6 (Figure 3c) represents a new structure type. It continues perfectly the transition from Cr_2AlB_2 via Cr_3AlB_4 to CrB_2 by insertion of additional zigzag chains of boron atoms in a trigonal-prismatic surrounding of Cr. In comparison to Cr_3AlB_4 a third zigzag chain amends the chain of hexagons to a double chain. Therefore, two of the three B atoms perform three B−B-bonds (1.707−1.738 Å). The central B−B−B angles (119.6−120.2°) are very close to the ideal values of 120°, while the deviations in the peripheral domain are more significant (116.2−121.9°). The same takes place for the Cr−B distances that change from 2.146 (Cr1−B1) to 2.329 Å (Cr2−B1). Even the tendencies for the Al-coordination are continued, including the elongation.

Systematic Tendencies in $CrAl(CrB_2)_n$ and Relation to the Binary Borides CrB, Cr_3B_4, Cr_2B_3, and CrB_2. The compounds $CrAl(CrB_2)_n$ are simple ternary variants of the binary borides in relation to the motifs of the boron subunits. They show the same structural units as they are realized in CrB (zigzag chain), Cr_3B_4 (chain of hexagons), and Cr_2B_3 (double chain of hexagons), respectively. A comparison of the structural features in $CrAl(CrB_2)_n$ (distances B−B and B−Cr, B−B−B angles) to the very precise data of Okada et al.[35] reveals the validity even for small details (B−B, Cr−B, and Cr−Cr distances, B−B−B angles).

The characterization of the first three members of the series $CrAl(CrB_2)_n$ allows us to estimate systematic variations of structural parameters. The longest B−B distances are observed for Cr_2AlB_2. The increase of the boron content shortens the distances in the central part, but in the peripheral part the longer distances are retained. As indicated by the B−B−B angles the reason is a shift of the outer B atom toward the Al. The B−Cr distances behave in the opposite way. The shortest ones are observed for Cr_2AlB_2 and the peripheral part (2.16−2.18 Å), the longest in the central part (2.27−2.33 Å). Both tendencies are observed in the same way for the binary borides (CrB, B−B 1.780 Å, Cr−B 2.186−2.220 Å; CrB_2, B−B 1.721 Å, Cr−B 2.320 Å; Cr_3B_4 and Cr_2B_3 are in between and similar to Cr_3AlB_4 and Cr_4AlB_6). The systematic variations extend to the Al atoms, too. With increasing boron content the distances Al−B are shortened while Al−Al and Al−Cr get longer. For the binary borides these relations are found for the capping Cr atom (CrB, 2.666 Å; Cr_3B_4, 2.680 Å; Cr_2B_3, 2.699 Å). The elongation of the bcc part is present in all compounds.

A first qualitative description of a homologous series $(CrB_2)_n(CrAl)_m$ was done by Jung et al.,[28] Jeitschko,[24,50] and Rogl.[51] The quantitative description is quite simple because of the close relation to the binary borides. Furthermore, the estimations of lattice parameters and interatomic distances can now be deduced from the series Cr_2AlB_2 ($n = 1$, $m = 1$), Cr_3AlB_4 ($n = 2$, $m = 1$), and Cr_4AlB_6 ($n = 3$, $m = 1$). According to the symmetry of the boride partial structure there are two space group types. With *n* as an even number, the space group is *Pmmm* while an odd number of *n* leads to space group *Cmmm*. The short lattice parameters, i.e., the metrics of the layers of BCr_6 prisms, show a systematic increase according to the increasing boron content. The long lattice parameter can be estimated from the incremental increase for each additional boron unit. Therefore, lattice parameters, space groups, and coordinates of the atoms can be derived completely from the systematic variations. Details are given for the members $n = 5$, Cr_5AlB_8, and $n = 6$, Cr_6AlB_{10}.[52]

MoAlB/WAlB. MoAlB was first described in 1942 by Halla and Thury[53] and characterized by X-ray methods and chemical analyses. They gave the composition $Mo_7Al_6B_7$, but the published diffraction pattern was identical to the data found later on. In 1966 Jeitschko communicated single crystal growth and structure refinement of MoAlB[24] using intensities of Weissenberg photographs and a trial-and-error refinement. The position of boron was deduced from the Mo positions assuming identical Mo−B distances. Jeitschko described the structure of MoAlB (Figure 3d) as a combination of a binary boride and an intermetallic compound. Similar to the structure of Cr_2AlB_2 the trigonal prisms BMo_6 are linked by two common rectangular planes to rods as it is also found in orthorhombic MoB[54] (*α*-MoB, CrB-type[35]). The intermetallic part represents a cut-out of bcc packing.

In 1995 Yu and Lundström presented crystal growth and structure refinement of a solid solution $Mo_{1-x}Cr_xAlB$ ($x = 0.31$).[55] Their results show that the Mo/Cr substitution keeps all structural features of MoAlB unchanged except the differences resulting from the metal atom's size. Okada el al.[38] reported on synthesis, single crystal growth, and hardness measurements on WAlB and solid solutions $Mo_{1-x}W_xAlB$, but no detailed structural parameters were given.

Recently, Albert et al. pointed out for the binary borides MoB_2 and WB_2[20] that the localization of B atoms is a problem in the case of 4d and especially 5d metals. Therefore, we have refined the structures of MoAlB and WAlB. Our results for MoAlB confirm the findings of Jeitschko and Okada. In comparison to the chromium borides all distances are slightly enlarged according to the larger size of Mo. Some small changes are observed for the intermetallic part. In contrast to the borides of

DOI: 10.1021/acs.inorgchem.5b00049
Inorg. Chem. 2015, 54, 6122−6135

3d metals with only one additional metal layer the bcc surrounding of Al is slightly compressed. Similar observations are made for $Ru_3Al_2B_2$.[56] The free refinement of the boron site results in Mo−B distances of 2.346 and 2.356 Å, a B−B distance of 1.810 Å, and a B−B−B angle within the zigzag chain of 117°.

The distances in WAlB are very similar to those of MoAlB. As already mentioned the localization of a light atom like boron besides a 5d metal is a problem. In the case of our data for WAlB the values for the displacement parameters of boron are in line with the expected values. This stands for a complete occupation and correct localization of the boron site. The B−B distance of 1.84 Å and a B−B−B angle within the zigzag chain of 115° are comparable to the value for tetragonal WB (1.883 Å, 111.1°) which were obtained from neutron data.[57]

Mn_2AlB_2/Fe_2AlB_2. The results for the refinements of Mn_2AlB_2 and Fe_2AlB_2 showed no peculiarities. Because of the slightly smaller size of Mn and Fe compared to that of Cr, the lattice parameters and distances are shortened. The elongation of the bcc part in direction [010] is confirmed. The results for Fe_2AlB_2 are in excellent agreement with the previous data given by Jeitschko.[27b] while there are significant differences to the data of Kuz'ma and Chaban.[27a] For Mn_2AlB_2 the earlier data[26] (B−B: 1.72 Å) fit quite well to our results.

Microhardness. Table 6 shows the microhardness values determined from single crystals in different orientations. Values were obtained from all compounds except Cr_4AlB_6. The microhardness for WAlB is based only on one measurement because of the small crystal size. The general tendency is the increase within the row of the 3d metals (Cr_2AlB_2 < Mn_2AlB_2 < Fe_2AlB_2). Furthermore, there is a strong increase within the same group following the atomic weight (Cr_2AlB_2 < MoAlB < WAlB) and with increasing boron content (Cr_2AlB_2 < Cr_3AlB_4). The very high values for WAlB were already reported by Okada et al.[38] They are characteristic for borides of 5d metals (TaB_2, WB_4, ReB_2, OsB_2)[4] and result from the strong M−M, M−B, and B−B bonding combined with the strong electron−electron repulsion of the core electrons.[4g]

Table 6. Hardness Values and Vickers Hardness H_V (in GPa) of MAB-Phases and Selected Binary Borides from Single Crystals

compd	hardness (min)	H_V	hardness (max)	H_V	ref
Cr_2AlB_2	622	6.0	720	7.0	this work
Mn_2AlB_2	734	7.0	1015	9.6	this work
Fe_2AlB_2	1200	11.6	1530	14.7	this work
Cr_3AlB_4	1560	15.0	2000	19.1	this work
MoAlB	1160	11.4	1385	13.6	this work
				10.3	ref 38c
WAlB			2200	21.7	this work
				19.3	ref 38c
CrB		21.1−22.8			ref 59
Cr_3B_4		21.9			ref 59
Cr_2B_3		22.4			ref 59
CrB_2		19.3−22.6			ref 59
CrB_4		26.1			ref 60
MnB	1816				ref 61
MnB_2	1240				ref 61
MnB_4		34.6		37.4	ref 62
FeB	1650				ref 63
FeB_4		43		70	ref 64

The variation of the microhardness is caused by the structural anisotropy. In general, the highest values are observed in the plane perpendicular to the zigzag chains, and the medium values are for the plane parallel to the intermetallic (or boride) partial structure. The lowest hardness is found for the plane perpendicular to the direction of the common trigonal faces of the BM_6 prisms. A detailed discussion of the hardness anisotropy will follow.

Formation and Stability of "MAB-Phases". Because we prepared single crystals for EDX and performed microhardness measurements we got qualitative information on formation and stability of the corresponding MAB-phases. It is striking that the solidified melts of the system Cr/Al/B frequently contain single crystals of binary borides. This is in agreement to the findings of Okada et al.[38] who obtained well-developed single crystals of the binary borides under very similar conditions, but with higher cooling rates. Probably the binary borides crystallize first and are transformed at lower temperatures into the MAB-phases. This can explain the formation of Al-inclusions in single crystals of Cr_3AlB_4, MoAlB, and Mn_2AlB_2. It can also be the reason for the problems of a reliable synthesis of Cr_4AlB_6. With M = Mn or Fe no binary borides are formed by crystallization from Al. Additionally, inclusions of CrB were observed in single crystals of Cr_2AlB_2. For Mn/Al/B a solid solution $Al_{1-x}Mn_xB_2$ is observed.[26,58] Furthermore, the MAB-phases become more and more reactive against hydrochloric acid with M = Mn and Fe. On the other hand no MAB-phases of titanium and vanadium are known while binary borides of titanium[65] and vanadium[66] are easily obtained from liquid aluminum. Furthermore, MAB-phases are known for the 4d metals Mo and Ru, while W is the only 5d metal. So the window of stability seems to be quite small with a maximum for 3d metals and group 6 metals.

DISCUSSION

Unified Building Block Principle for Binary and Ternary Metal Borides (MAB-Phases) on the Basis of Metal 4^4-Nets. Recently, we published a general description of MAX-phases $M_{n+1}AX_n$ on the basis of NaCl-fragments MX and additional intermetallic layers MA in between.[32b] According to the common features, layers of closest packed metal atoms are central and lead to hexagonal structures.

The systematics of ternary borides are obvious and were already discussed in a qualitative way by Jeitschko,[24,50] Jung,[28] and Rogl.[51] A unifying concept for the description of binary and ternary borides and boridecarbides including space groups, lattice parameters, and atomic sites is based on the stacking of 4^4-nets of the metal atoms. This concept was developed for the description of niobium boridecarbides $Nb_xB_yC_z$,[67] where the carbide part represents a cut-out of the rocksalt structure, i.e., an fcc packing of Nb and C in all octahedral voids. Now we extend it to the consideration of ternary borides based on 4^4 nets where the intermetallic part represents a bcc-like arrangement. Furthermore, we include the two different types of arrangements of the boride partial structure, i.e., parallel orientation leading to orthorhombic structures and alternating orthogonal orientation that results in tetragonal symmetry.

The fundamental building units can be reduced to two different types of stacking for a quadratic 4^4-net of metal atoms (Scheme 1). The bcc-unit (ternary borides) and/or the CTM_6-octahedra (boridecarbides) are yielded if the subsequent 4^4-net is placed above/below the center of the square. In that way there results a cubic surrounding for the metal atoms of the central

DOI: 10.1021/acs.inorgchem.5b00049
Inorg. Chem. 2015, 54, 6122−6135

Scheme 1. Generation of Carbide/bcc and Boride Units by Stacking of 4^4-Nets

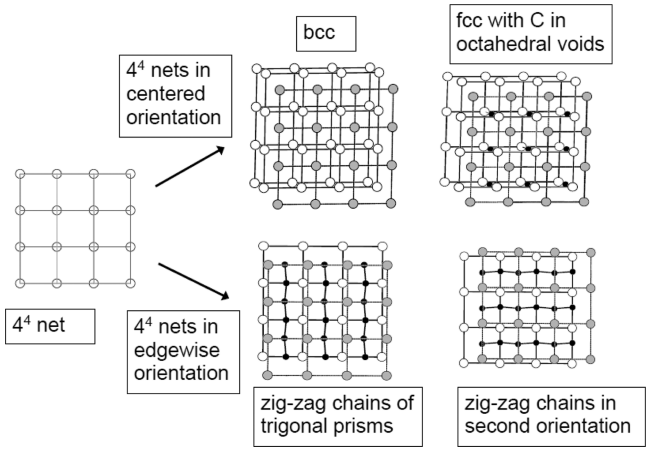

layer and an octahedral void for center of the square. The tetragonal symmetry is maintained.

Trigonal prisms BTM_6 are obtained by placing the adjacent net over the square's edge. The number of trigonal-prismatic voids is twice the number of nods of the net, i.e., the number of metal atoms in a layer. The symmetry of the layer (or more precisely the set of layers) is reduced from tetragonal to orthorhombic. With two metal layers and filled voids there results the composition M_2B_2 and a zigzag chain of boron atoms, i.e., the motif of the monoboride CrB. Additional metal layers representing a fragment $(MB_2)_n$ amend the zigzag chain to a chain of hexagons (M_3B_4), or double chain of hexagons (M_2B_3).

Ideal values for the voids are obtained for special distances between subsequent 4^4 nets and a pseudotetragonal metric of the orthogonal unit cells. With τ as the mesh size of the 4^4 net the idealized distances are $\sqrt{3}/2\ \tau$ for the trigonal prisms, $1/2\ \tau$ for the octahedral voids (fcc), and $\sqrt{2}/2\ \tau$ for the intermetallic bcc fragment.

For the boride partial structure it is assumed for a start that always the same edges of the square, i.e., left/right or top/bottom, are capped by the subsequent 4^4-net. Therefore, the zigzag chains or chains of hexagons run all into the same direction. With a parallel arrangement of the boride motifs orthorhombic structures are obtained, because the tetragonal symmetry of the 4^4-nets is broken by the trigonal prisms. Scheme 2 gives an overview of structures which can be combined in that way. According to the different numbers of metal layers in the trigonal-prismatic part (x) and the bcc part (y) the corresponding compositions are obtained. For $y = 1$, and $x = 2$, 3, or 4, the resulting compounds are Cr_2AlB_2, Cr_3AlB_4, and Cr_4AlB_6, respectively. The binary borides result for $y = 0$. The examples of MoAlB ($x = 2$, $y = 2$) and $Ru_3Al_2B_2$ ($x = 2$, $y = 3$, Ru in central bcc-layer) show that values of $y > 1$ are possible, too. Changing the distance of the 4^4 nets realizes the features of an fcc packing (see above) where octahedral voids can be occupied. Now the boridecarbides of niobium and molybdenum as well as Nb_2BN[68] and $Pr_3Si_2C_2$ (disordered C_2-units in octahedral voids)[69] fit also to this scheme.

This building block principle can also be used to predict the complete crystal structure of any representative. The lattice parameters can be estimated from an incremental system derived from the binary borides and intermetallics or metallic radii. The space group is only determined by the combination of x and y. It can be shown that a difference of ± 2 for x and y does not change the space group. Therefore, four cases (and space groups) can be distinguished, according to even or odd numbers for x and y. These space groups are *Cmcm* (x and y even), *Immm* (x odd, y even), *Cmmm* (x even, y odd), and *Pmmm* (x and y odd). Finally, the atomic coordinates can be derived from the evaluation of the systematic variations (for example discussed for the series $(CrB_2)_nCrAl$ with $n = 4$ and 5).[52]

For the examples in Scheme 1 the parallel arrangement of the boron subunits is assumed. This results in orthorhombic structures. However, for the monoborides CrB, MoB, and WB the existence of a second tetragonal phase is known.[37,70] This structure can be derived from the orthorhombic structure by a 90°-rotation of the zigzag chain leading to a doubling of the lattice parameter and space group $I4_1/amd$. Using the description with 4^4-nets it corresponds a capping the other side of the square. Furthermore, Jung and Petry described the tetragonal structure of Ru_2ZnB_2 ($I4_1/amd$, $a = 2.946$ Å, $c = 22.90$ Å)[28] which shows the same feature. Therefore, we have extended the unified concept to structures with orthogonal boron subunits compiled

Scheme 2. Orthorhombic Representatives (Parallel Orientation of Boron Units), See Text

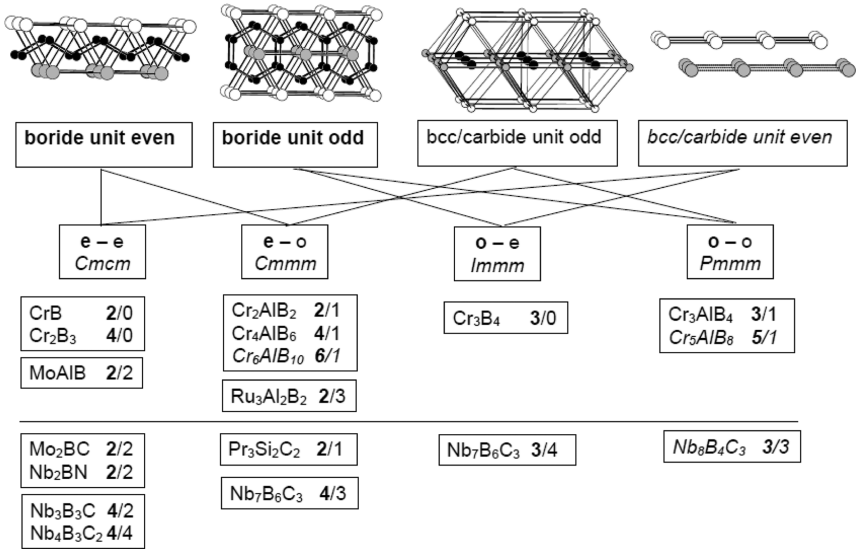

DOI: 10.1021/acs.inorgchem.5b00049
Inorg. Chem. 2015, 54, 6122–6135

Scheme 3. Tetragonal Representatives (Orthogonal Orientation of Boron Units), See Text

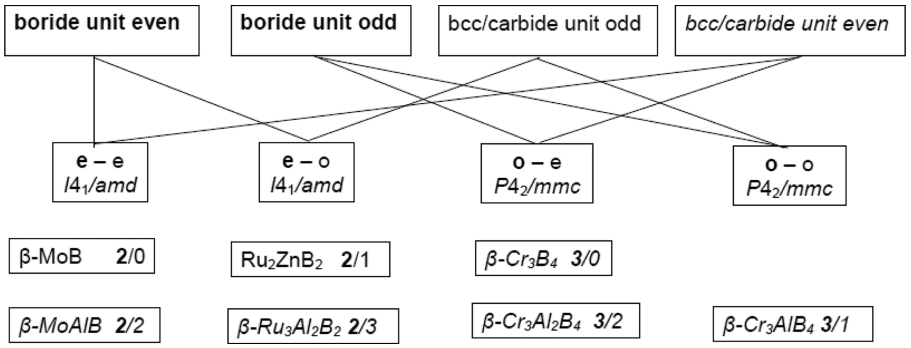

in Scheme 3. It can be shown that two different tetragonal structures are obtained. For even numbers of x (for example, β-MoB, $x = 2$, $y = 0$; Ru_2ZnB_2, $x = 2$, $y = 1$), it always results in a structure with space group $I4_1/amd$. For odd numbers of x, the space group is $P4_2/mmc$, independent from y. Up to now there is no example for that case, but structure models can be set up for these ternary compounds, too. The lattice parameters may be derived from the known orthorhombic representatives. The tetragonal a-axis is the average of the two short axes of the orthorhombic unit cell; the tetragonal c-axis corresponds to the long axis (identical for $P4_2/mmc$, doubled for $I4_1/amd$).[71]

The homologous series with its generalized description requires special conditions for symmetry and metrics. In this case, where distinct layers are stacked in a 3D periodic crystal structure, the symmetry of the layer must fit to the corresponding plane of the space group. The symmetry of the layer is described by one of the 80 two-sided plane groups.[72]

According to Scheme 2 the four different types of layers are assigned to the two-sided layer groups. They are as follows: odd boride unit $pmmm$ ($p2/m2/m2/m$, No. 23), even boride unit $pmma$, ($p2_1/m2/m2/a$, No. 43); odd bcc/carbide unit $p4/mmm$ ($p4/m2/m2/m$, No. 53), even bcc/carbide unit $p4/nmm$ ($p4/n2_1/m2/m$, No. 63). The matching of space group and layer group is fulfilled in all cases and comprises two ($Pmmm$), four ($Immm$, $Cmmm$, $Cmcm$, $P4_2/mmc$), or eight ($I4_1/amd$) layers. A second condition refers to the metric of the layers. The stacking of different layers requires that all symmetry elements perpendicular to the layer can be combined. This is fulfilled because for all four layers the symmetry of the straight lines $00z$, $0\,^1/_2z$, $\,^1/_20z$, and $\,^1/_2\,^1/_2z$ (defining the unit vector of the 4^4-net as unity in directions x and y and the stacking direction as z-axis) is $mm2$ or one of its super groups, so the metrics of all layers fit to each other. Finally, the transition between the layers must be structurally reasonable. In this case it means that the free rectangular faces of the trigonal prisms are centered by the next 4^4-net. This generates an additional vector of $\,^1/_2\,^1/_20$, which amends the translational components of the layers (if there are any) to those of the space group.

In principle, this building concept can be extended by consideration of dissimilar boride units (for example Nb_5B_6 with zigzag chains and chains of hexagons),[40] fragments of boron chains, or combinations of boride, carbide, and bcc units. The structures of $Ru_8Zn_5B_8$ and $Ru_9Al_5B_6$[28] can be seen as a transition between the tetragonal variants and borides with chain fragments. The combination results in an orthogonal arrangement of B_4-fragments of the zigzag chains. Even the structure of $Ni_{12}AlB_8$[15] with pentamers and isolated boron atoms can be classified like this. A recent example is Ni_3ZnB_2[73] with a parallel arrangement of B_4 chain fragments separated by Zn layers. This can be seen as a link between borides with zigzag chains and borides with chain fragments. However, according to the symmetry reduction the description with 4^4-nets is no longer possible.

CONCLUSIONS

The crystal structure of Cr_4AlB_6 showed that the systematics of binary borides with compositions between MB (B−B zigzag chains) and MB_2 (planar hexagonal nets of boron atoms) can be transferred to ternary representatives $(MB)_2Al(MB_2)_x$. A generalized structure principle might be useful for the investigation of boride-based materials by electron microscopy. Small particles or interfaces of ceramics or composites can be investigated by HRTEM or electron diffraction. According to symmetry and lattice parameters a detailed structure model can be derived even for very small regions, and its properties can be estimated. Interesting material properties of ternary transition metal borides result from the extremely high thermal, chemical, and mechanical stability of the corresponding binary borides. Similar to the closely related ternary carbides (MAX-phases) the marked anisotropy of the structures, i.e., alternating layers of intermetallic and boride subunits, offers unique properties.

In comparison to that of the MAX-phases the number of MAB-phases is much smaller. The reason is that the variation of the transition metal and especially the main group metal "A" is much more restricted. Up to now MAB-phases are characterized only for A = Al, Zn (one example: Ru_2ZnB_2), and Ru (one example: $Ru_3Al_2B_2$, Ru also in bcc layers). Nevertheless, the structural diversity and complexity of MAB-phases is more distinctive than actually known for MAX-phases, because MAB-phases have more degrees of freedom. The carbide partial structure of MAX-phases represents a (111)-cut-out of rock salt which is separated by one single "A"-layer. The thickness of the carbide part is the only variable. In contrast to this, MAB-phases have three variables, i.e., the thickness of the boride part, and the number of metal layers between the boride part and the orientation of the boron subunits. The latter results from the fact that the boron subunits are based on zigzag chains, which can be orientated in a parallel or an orthogonal way.

All three aspects of variability are considered in our generalized scheme for MAB-phases and related boridecarbides, which uses the combination of 4^4-nets of M and A. The space group symmetry for each type can be derived directly from the number of layers in the two subunits. The boride part determines the crystal system. With a parallel alignment of zigzag chains there are four orthorhombic space groups; with an orthogonal orientation there are two tetragonal space groups. The

DOI: 10.1021/acs.inorgchem.5b00049
Inorg. Chem. 2015, 54, 6122−6135

intermetallic part (or carbidic part for boridecarbides) is compatible with both crystal systems. Lattice parameters and coordinates of the atoms can be derived from the distances in binary or ternary references.

From liquid aluminum we have obtained single crystals for the series $Cr_2AlB_2(CrB_2)_x$ (x = 0, 1, 2), M_2AlB_2 (M = Cr, Mn, Fe), and MAlB (M = Mo, W). Detailed X-ray investigations revealed systematic interconnections between boron content (i.e., size of the boride partial structure) and transition metal (i.e., group number of the 3d metal and 3d/4d/5d metal). Deviations from expected values are usually caused by inadequate treatment of the X-ray data like intensity measurement or absorption correction. With an appropriate sample preparation and calibration all compositions were confirmed by quantitative electron microprobe analysis (EDX) including the boron content. Furthermore, the access to single crystals allowed the measurement of microhardness values. In general, the hardness of MAB-phases is higher than for the similar MAX-phases, but according to preliminary findings the structural anisotropy does not result in a corresponding anisotropy of the mechanical properties as was found for the MAX-phases.

■ ASSOCIATED CONTENT

Supporting Information

Experimental and calculated powder XRD patterns, and additional SEM pictures. Crystallographic data in CIF format. The Supporting Information is available free of charge on the ACS Publications website at DOI: 10.1021/acs.inorgchem.5b00049.

■ AUTHOR INFORMATION

Corresponding Author

*E-mail: harald.hillebrecht@ac.uni-freiburg.de. Phone: 0049-761-203 6131. Fax: 0049-761-203 6102.

Notes

The authors declare no competing financial interest.

■ DEDICATION

Dedicated to Prof. Dr. G. Thiele.

■ REFERENCES

(1) Kieffer, R.; Benesovsky, F. *Hartstoffe*; Springer-Verlag: Wien, 1963.
(2) Toth, L. E. *Transition Metal Carbides and Nitrides*; Academic Press: New York, 1971.
(3) *Boron and Refractory Borides*; Matkovich, V. I., Ed.; Springer Verlag: Berlin, 1977.
(4) (a) Chung, H.-Y.; Weinberger, M. B.; Levine, J. B.; Kavner, A.; Yang, J.-M.; Tolbert, S. H.; Kaner, R. B. *Science* **2007**, *316*, 436−439. (b) Qin, J.; He, D.; Wang, J.; Fang, L.; Lei, L.; Li, Y.; Hu, J.; Kou, Z. *Adv. Mater.* **2008**, *20*, 4780−4783. (c) Cumberland, P. W.; Weinberger, M. B.; Gilman, J. J.; Clark, S. M.; Tolbert, S. H.; Kaner, R. B. *J. Am. Chem. Soc.* **2005**, *127*, 7264−7265. (d) Chen, X.-Q.; Fu, C. L.; Krcmar, S.; Painter, G. S. *Phys. Rev. Lett.* **2008**, *100*, 19640. (e) Koehler, M. R.; Keppens, V.; Sales, B. C.; Jin, R.; Mandrus, D. *J. Phys. D: Appl. Phys.* **2009**, *42*, 095414. (f) Simunek, A. *Phys. Rev. B* **2009**, *80*, 060103. (g) Gu, F. Q.; Krauss, G.; Steurer, W. *Adv. Mater.* **2008**, *20*, 3620−3626. (h) Okada, S.; Kudou, K.; Higashi, I.; Lundström, T. *J. Cryst. Growth* **1993**, *128*, 1120−1124. (i) Mohammadi, R.; Xie, M.; Weaver, B. E.; Young, M. T.; Tolbert, S. H.; Kaner, R. B. *Proc. Natl. Acad. Sci. U.S.A.* **2011**, *108*, 10958−10962.
(5) (a) Barsoum, M. W. *Prog. Solid State Chem.* **2000**, *28*, 201. (b) Zhang, H. B.; Bao, Y. W.; Zhou, Y. C. *J. Mater. Sci. Technol.* **2009**, *25*, 1. (c) Eklund, P.; Beckers, M.; Jansson, U.; Högberg, H.; Hultman, L. *Thin Solid Films* **2010**, *518*, 1851−1878.
(6) (a) Villars, P.; Calvert, L. D. *Pearson's Handbook, Crystallographic Data for Intermetallic Phases*; ASM International: Materials Park, OH, 1997. CD-ROM version 2.0, 2008. (b) ICSD database: http://icsd.fiz-karlsruhe.de/icsd/.
(7) Nowotny, H.; Rogl, P. In ref 3, p 413.
(8) Rogl, P. In *Inorganic Reactions and Methods*; Hagen, A., Ed.; Wiley: New York, 1991; Vol. *13*, pp 85−167.
(9) Gladysevskii, E. I.; Fedorov, T. F.; Kuz'ma, Y. B.; Skolozdra, R. V. *Powder Metall. Met. Ceram.* **1966**, *5*, 305−309.
(10) Rieger, M.; Nowotny, H.; Beneshovsky, F. *Monatsh. Chem.* **1966**, *97*, 378−382.
(11) Jedlicka, H.; Benesovsky, F.; Nowotny, H. *Monatsh. Chem.* **1969**, *100*, 844−850.
(12) Rogl, P.; Benesovsky, F.; Nowotny, H. *Monatsh. Chem.* **1972**, *103*, 965−989.
(13) Kotzott, D.; Ade, M.; Hillebrecht, H. *Solid State Sci.* **2008**, *10*, 291−302.
(14) Fokwa, B. P. T.; von Appen, J.; Dronskowski, R. *Chem. Commun.* **2006**, 3612−3614.
(15) Ade, M.; Kotzott, D.; Hillebrecht, H. *J. Solid State Chem.* **2010**, *183*, 1790−1797.
(16) Fokwa, B. P. T.; Hermus, M. *Angew. Chem.* **2012**, *124*, 1734−1737; *Angew. Chem., Int. Ed.* **2012**, *51*, 1702−1705.
(17) Bertaut, F.; Blum, P. *Acta Crystallogr.* **1951**, *4*, 66−67.
(18) Hendricks, S. B.; Kosting, P. R. *Z. Kristallogr.* **1930**, *74*, 511−533.
(19) Kiessling, R. *Acta Chem. Scand.* **1947**, *1*, 893−916.
(20) Frotscher, M.; Klein, W.; Bauer, J.; Fang, C.-M.; Halet, J.-F.; Senyshyn, A.; Baehtz, C.; Albert, B. *Z. Anorg. Allg. Chem.* **2007**, *633*, 2626−2630.
(21) La Placa, S. J.; Post, B. *Acta Crystallogr.* **1962**, *15*, 97−99.
(22) Kuz'ma, Y. B. *Sov. Phys. Crystallogr.* **1970**, *15*, 312−314.
(23) Kuz'ma, Y. B.; Svarichevskaya, S. I. *Sov. Phys.-Crystallogr.* **1972**, *17*, 569−571.
(24) Jeitschko, W. *Monatsh. Chem.* **1966**, *97*, 1472−1476.
(25) (a) Kuz'ma, Y. B.; Krypyakevich, P. I.; Chaban, N. F. *Dopov. Akad. Nauk Ukr. RSR, Ser. A: Fiz.-Mat. Tekh. Nauki* **1972**, 1118. (b) Chaban, N. F.; Kuz'ma, Y. B. *Inorg. Mater.* **1973**, *9*, 1696−1698.
(26) Becher, H. J.; Krogmann, K.; Peisker, E. *Z. Anorg. Allg. Chem.* **1966**, *344*, 140−147.
(27) (a) Kuzma, Y. B.; Chaban, N. F. *Inorg. Mater.* **1969**, *5*, 321−322. (b) Jeitschko, W. *Acta Crystallogr., Sect. B* **1969**, *25*, 163−165.
(28) Jung, W.; Petry, K. *Z. Kristallogr.* **1988**, *18*, 153−154.
(29) Telle, R.; Momozawa, A.; Music, D.; Schneider, J. M. *J. Solid State Chem.* **2006**, *179*, 2850−2857.
(30) Tan, X.; Chai, P.; Thompson, C. M.; Shatruk, M. *J. Am. Chem. Soc.* **2013**, *135*, 9553−9557.
(31) Chai, P.; Stoian, S. A.; Tan, X.; Dube, P. A.; Shatruk, M. *J. Solid State Chem.* **2015**, *224*, 52−61.
(32) (a) Etzkorn, J.; Ade, M.; Hillebrecht, H. *Inorg. Chem.* **2007**, *46*, 1410−1418. (b) Etzkorn, J.; Ade, M.; Hillebrecht, H. *Inorg. Chem.* **2007**, *46*, 7646−7653. (c) Etzkorn, J.; Ade, M.; Kotzott, D.; Kleczek, M.; Hillebrecht, H. *J. Solid State Chem.* **2009**, *182*, 995−1002. (d) Kotzott, D.; Hillebrecht, H. *Z. Kristallogr. Suppl.* **2009**, *29*, 79. (e) Kotzott, D.; Hillebrecht, H. *J. Alloys Compd.* **2010**, *494*, 88−93. (f) Etzkorn, J.; Hillebrecht, H. *J. Solid State Chem.* **2008**, *181*, 1342−1346.
(33) (a) Hillebrecht, H.; Ade, M. *Angew. Chem.* **1998**, *110*, 981−983; *Angew. Chem., Int. Ed.* **1998**, *37*, 935−938. (b) Kotzott, D.; Ade, M.; Hillebrecht, H. *J. Solid State Chem.* **2009**, *182*, 538−546. (c) Kotzott, D.; Ade, M.; Hillebrecht, H. *J. Solid State Chem.* **2010**, *183*, 2281−2289.
(34) Stadelmaier, H.; Burgess, R. E.; Davis, H. H. *Metall* **1966**, *20*, 225−226.
(35) Okada, S.; Atoda, I.; Higashi, I. *J. Solid State Chem.* **1987**, *68*, 61−67.
(36) (a) Ade, M. Diploma Thesis, University Freiburg, 1994. (b) Ade, M. Ph.D. thesis, University Freiburg, 1997.
(37) Rudy, E.; Benesovsky, F.; Toth, L. *Z. Metallkd.* **1963**, *54*, 345−353.
(38) (a) Okada, S. *Kokushikan Daigaku Kogakubu Kiyo* **1998**, *31*, 7−12. (b) Zhang, Y.; Okada, S.; Atoda, T.; Yamabe, T.; Yasumori, I. *Yogyo*

DOI: 10.1021/acs.inorgchem.5b00049
Inorg. Chem. 2015, 54, 6122−6135

Kyokaishi **1987**, *95*, 10−16. (c) Okada, S.; Iizumi, K.; Kudaka, K.; Kudou, K.; Miyamata, M.; Yu, Y.; Lundström, T. *J. Solid State Chem.* **1997**, *133*, 36−43.
(39) Cenzual, K.; Gelato, L. M.; Penzo, M.; Parthé, E. *Acta Crystallogr., Sect. B* **1991**, *47*, 433−439.
(40) (a) Bolmgren, H.; Lundström, T.; Tergenius, L. E.; Okada, S.; Higashi, I. *J. Less-Common Met.* **1999**, *161*, 341−345. (b) Spear, K. E.; Gilles, P. W. *High Temp. Sci.* **1969**, *1*, 86−97.
(41) Sheldrick, G. M. *SHELXTL Program Package*; University of Göttingen: Göttingen, Germany, 1997.
(42) *Program XAREA, XRED*; Stoe Cie: Darmstadt, Germany.
(43) *XSHAPE*; Stoe Cie: Darmstadt, Germany.
(44) (a) Ade, M.; Hilllebrecht, H. Unpublished results. (b) Adasch, V.; Hess, K.-U.; Ludwig, T.; Vojteer, N.; Hillebrecht, H. *Chem.—Eur. J.* **2007**, *13*, 3450−3458. (c) Adasch, V.; Schroeder, M.; Kotzott, D.; Ludwig, T.; Vojteer, N.; Hillebrecht, H. *J. Am. Chem. Soc.* **2010**, *132*, 13723−13732. (d) Pediaditakis, A.; Haseloff, S.; Hillebrecht, H. *Solid State Sci.* **2011**, *13*, 1465−1472. (e) Schroeder, M.; Schlöder, T.; Lehner, A. J.; Hillebrecht, H. *Inorg. Chem.* **2010**, *49*, 3130−3140. (f) Ludwig, T.; Pediaditakis, A.; Sagawe, V.; Hillebrecht, H. *J. Solid State Chem.* **2013**, *204*, 113−122.
(45) DIN EN 6507.
(46) (a) Kozlov, E. Y.; Semukhin, B. S.; Rubinovich, L. M.; Shtern, D. M. *Phys. Met. Metallogr.* **1983**, *56*, 113−116. (b) Oforka, N. C.; Haworth, C. W. *Scand. J. Metall.* **1987**, *16*, 184−188.
(47) Kallel, A. *C. R. Seances Acad. Sci., Ser. B* **1969**, 268−455.
(48) Braun, J.; Ellner, M.; Predel, B. *J. Alloys Compd.* **1987**, *183*, 444−448.
(49) Mykhalenko, S. I.; Babizhetskii, V. S.; Kuz'ma, Y. B. *J. Solid State Chem.* **2004**, *177*, 439−443.
(50) Jeitschko, W.; Nowotny, H.; Benesovsky, F. *Monatsh. Chem.* **1963**, *94*, 565−568.
(51) Rogl, P. In *Modern Perspectives in Inorganic Crystal Chemistry*; Parthé, E., Ed.; 19th Course International School of Crystallography: Erice, Italy, 1992.
(52) Cr_5AlB_8: *Pmmm*, a = 2.964 Å, b = 3.050 Å, c = 13.26 Å; B1, 2*r* 0 0.5 0.065; B2, 2*t* 0.5 0.5 0.132; B3, 2*t* 0.5 0.5 0.263; B4, 2*r* 0 0.5 0.333; Cr1, 2*b* 0.5 0 0.390; Cr2, 2*q* 0 0 0.197; Cr3, 1*b*; Al; 1*g*. Cr_6AlB_{10}: *Cmmm*, a = 2.968 Å, b = 31.78 Å, c = 3.070 Å; B1, 4*j* 0.5 0.1568 0.5; B2, 4*j* 0.5 0.1817 0.5; B3, 4*j* 0 0.2360 0.5; B4, 4*j* 0.5 0.1000 0.5; B5, 4*j* 0 0.0706 0.5; Cr1, 4*i* 0.5 0.0519 0; Cr2, 4*i*, 0 01253 0; Cr3, 4*i* 0.5 0.2088 0; Al, 2*d*.
(53) Halla, F.; Thury, W. *Z. Anorg. Allg. Chem.* **1942**, *249*, 229−237.
(54) Rudy, E.; Benesovsky, F.; Toth, L. *Z. Metallkd.* **1963**, *54*, 345−353.
(55) Yu, Y.; Lundström, T. *J. Alloys Compd.* **1995**, *226*, 5−9.
(56) Jung, W.; Schweitzer, K. *Z. Kristallogr.* **1988**, *178*, 109−110.
(57) Kayhan, M.; Hildebrandt, E.; Frotscher, M.; Senyshyn, A.; Hofmann, K.; Alff, L.; Albert, B. *Solid State Sci.* **2012**, *14*, 1656−1659.
(58) Confirmed by our EDX analyses.
(59) Okada, S.; Kudou, K.; Iizumi, K.; Kudaka, K.; Higashi, I.; Lundström, T. *J. Cryst. Growth* **1996**, *166*, 429−435.
(60) Kappschneider, A.; Litterscheid, C.; Kurzman, J.; Seshadri, R.; Albert, B. *Inorg. Chem.* **2013**, *52*, 540−542.
(61) Cely, A.; Tergenius, L.-E.; Lundström, T. *J. Less-Common Met.* **1978**, *61*, 193−198.
(62) Gou, H.; Alexander, A.; Tsirlin, A. A.; Bykova, E.; Abakumov, A. M.; Van Tendeloo, G.; Richter, A.; Ovsyannikov, S. V.; Kurnosov, A. V.; Trots, D. M.; Konopkov, Z.; Liermann, H. P.; Dubrovinsky, L.; Dubrovinskaia, N. *Phys. Rev. B* **2014**, *89*, 064108.
(63) Kunitskii, Yu. A.; Marek, E. V. *Poroshk. Metall.* **1971**, *99*, 56−59; English translation: *Powder Metall Met. Ceram.* **1971**, *10*, 216−218.
(64) Gou, H.; Dubrovinskaia, N.; Bykova, E.; Tsirlin, A. A.; Kasinathan, D.; Schnelle, W.; Richter, A.; Merlini, M.; Hanfland, M.; Abakumov, A. M.; Batuk, D.; Van Tendeloo, G.; Nakajima, Y.; Kolmogorov, A. N.; Dubrovinsky, L. *Phys. Rev. Lett.* **2013**, *111*, 157002.
(65) Higashi, I. *J. Cryst. Growth* **1970**, *7*, 251−253.
(66) S. Okada, S.; Shishido, T.; Kanari, H.; Nakajima, K. *Pac. Sci. Rev.* **2008**, *10*, 39−44.
(67) Hillebrecht, H.; Gebhardt, K. *Angew. Chem.* **2001**, *113*, 1492−1495; *Angew. Chem., Int. Ed.* **2001**, *40*, 1445−1447.
(68) (a) Rogl, P.; Klesnar, H. P.; Fischer, P. *J. Am. Ceram. Soc.* **1988**, *71*, C450−452. (b) Rogl, P.; Klesnar, H. P.; Fischer, P.; Chevalier, B.; Buffat, B.; Demazeau, G.; Etourneau, J. R. *J. Mater. Sci. Lett.* **1988**, *7*, 1229−1230.
(69) Jeitschko, W.; Gerdes, M. H.; Witte, A. M.; Rodewald, U. C. *J. Solid State Chem.* **2001**, *156*, 1−9.
(70) (a) Papesch, G.; Nowotny, H.; Benesovsky, F. *Monatsh. Chem.* **1973**, *104*, 933−942. (b) Kiessling, R. *Acta Chem. Scand.* **1950**, *4*, 209−227. (c) Steinitz, R.; Binder, J.; Moskovitz, D. *Trans. Am. Inst. Min., Metall. Pet. Eng.* **1952**, *194*, 983−987. (d) Haschke, H.; Nowotny, H.; Benesovsky, F. *Monatsh. Chem.* **1966**, *97*, 1459−1468.
(71) "β-MoAlB": x = 2, y = 2, $I4_1/amd$, a = 3.15 Å, c = 27.96 Å; Mo, 8*e*, 0.5 0.75 0.155; Al, 8*e*, 0 0.25 0.210, B, 8*e*, 0 0.25 0.013. β-$Ru_3Al_2B_3$: $I4_1/amd$, a = 3.15 Å, c = 36.10 Å, x = 2, y = 3; Ru1, 4*b*; Ru2, 8*e*, 0 0.75 0.0325; Al, 8*e*, 0 0.75 0.0786; B, 8*e*, 0 0.75, 0.0122. β-Cr_3B_4: x = 3, y = 0, $P4_2/mmc$, a = 2.96 Å, c = 13.01 Å; Cr1, 2*a*; Cr2, 4i, 0 0.5 0.190; B1, 4*i*, 0.5 0 0.133; B2, 4*h*, 0.5 0.5 0.066. β-Cr_3AlB_4, x = 3, y = 1, $P4_2/mmc$, a = 2.96 Å, c = 19.61 Å; Cr1, 2*c*; Cr2, 4*h*, 0.5 0.5 0.166; B1, 4*i*, 0.5 0 0.046; B2, 4*g*, 0 0 0.092. β-$Cr_3Al_2B_4$: x = 3, y = 2, $P4_2/mmc$, a = 2.96 Å, c = 22.91 Å; Cr1, 2*a*; Cr2, 4*i*, 0 0.5 0.126; Al, 4*i*, 0.5 0 0.205; B1, 4*i*, 0.5 0 0.088; B2, 4*h*, 0.5 0.5 0.044.
(72) (a) Weber, L. *Z. Kristallogr.* **1929**, *70*, 309−327. (b) Holser, W. T. *Z. Kristallogr.* **1958**, *110*, 266−281. (c) Shubnikov, A. V.; Koptsik, V. A. *Symmetry in Science and Art*; Plenum Press: New York, 1977.
(73) Malik, Z. P.; Sologub, O.; Grytsiv, A.; Giester, G.; Rogl, P. F. *Inorg. Chem.* **2011**, *50*, 7669−7675.

DOI: 10.1021/acs.inorgchem.5b00049
Inorg. Chem. 2015, 54, 6122−6135